ELSEVIER

Chemical Engineering Science 58 (2003) 5339–5347

Chemical Engineering Science

www.elsevier.com/locate/ces

Electrophoresis of a spheroid along the axis of a cylindrical pore

Jyh-Ping Hsu[a,*], Shih-Hsing Hung[a], Chen-Yuan Kao[a], Shiojenn Tseng[b]

[a] *Department of Chemical Engineering, National Taiwan University, Taipei 10617, Taiwan, ROC*
[b] *Department of Mathematics, Tamkang University, Tamsui, Taipei 25137, Taiwan, ROC*

Received 3 March 2003; received in revised form 24 July 2003; accepted 5 September 2003

Abstract

The boundary effect in electrophoresis can play an important role in applications of practical significance; typical example includes the electrophoresis in a narrow space and that of a concentrated dispersion. This effect is investigated by analyzing the electrophoresis of a spheroid along the axis of an infinite non-conducting cylinder in this study for the case of low surface potential. In particular, the effects of particle aspect ratio, the ratio (linear size of particle/radius of pore), double layer thickness, and the charged conditions on particle surface on the electrophoretic behavior of a particle are discussed. Several interesting results are observed. For example, if the volume of a particle is fixed, its electrophoretic mobility has a local maximum as its aspect ratio varies. Also, if wall effect is important, the relative magnitudes of the electrophoretic mobility of a particle follow the order prolate $<$ sphere $<$ oblate, and the reverse is true if it is unimportant.

Keywords: Electrophoresis in cylindrical pore; Spheroid; Constant surface potential; Constant surface charge density

1. Introduction

Electrophoresis is one of the basic analytical tools for both quantification and separation of a dispersed system. It is based on the fact that charged entities would migrate toward one of the two electrodes of an applied electric field. Smoluchowski pioneered the theoretical analysis on this phenomenon (Hunter, 1989). He considered the case when a rigid particle is placed in an infinite fluid. Under the conditions of steady state, low electrical potential, constant particle surface property, and the linear size of the particle is much larger than the thickness of double layer surrounding it, Smoluchowski was able to show that the electrophoretic velocity of the particle is proportional to the product of its zeta potential and the applied electric field (Morrison, 1970). The ratio (electrophoretic velocity/applied electric field) is defined as the electrophoretic mobility of the particle. Although Smoluchowski's result provides a concise analytical expression for the dependence of electrophoretic velocity (or mobility) on the applied electric field, some of its assumptions may need modification to meet conditions of practice significance. One of these is the liquid surrounding a particle is infinite, i.e., the boundary effect is negligible. This effect can be significant; for example, in the case the electrophoresis is conducted in a narrow space such as a pore in a membrane or in the case the effect of neighboring particles should be considered such as a concentrated dispersion.

Attempts have been made in the literature to simulate the boundary effect of electrophoresis for various types of geometry. These include, for example, a sphere moves parallel to a plane (Keh and Anderson, 1985; Keh and Chen, 1988; Ennis and Anderson, 1997), normal to a plane (Keh and Anderson, 1985; Ennis and Anderson, 1997; Keh and Lien, 1989; Keh and Jan, 1996; Chih et al., 2002; Tang et al., 2001), along the axis of a cylinder (Keh and Anderson, 1985; Ennis and Anderson, 1997; Keh and Chiou, 1996; Shugai and Carnie, 1999), electrophoresis of multiple spheres and spheroids (Keh and Chen, 1989a,b; Keh and Yang, 1990; Chen and Keh, 1992; Loewenberg and Davis, 1995; Sun and Wu, 1995; Shugai et al., 1997), a body of revolution moves normal to a plane (Feng and Wu, 1994), a sphere at the center of a spherical cavity (Zydney, 1995; Lee et al., 1997, 1998; Chu et al., 2001), an infinite cylinder with its axis parallel to a planar wall (Keh et al., 1991), a sphere moving axially toward a circular hole or disk (Keh and Lien, 1991).

In this study, we consider the electrophoresis of a spheroid along the axis of an infinitely long, non-conducting and

* Corresponding author. Tel.: +886-2-2363-7448; fax: +886-2-2362-3040.
E-mail address: jphsu@ccms.ntu.edu.tw (J.-P. Hsu).

0009-2509/$ - see front matter © 2003 Elsevier Ltd. All rights reserved.
doi:10.1016/j.ces.2003.09.013

uncharged cylindrical pore. Choosing spheroidal geometry has the advantage that it is capable of simulating a wide class of particles by varying the relative length of its major and minor axes. We consider two types of charged conditions on particle surface: constant electrical potential and constant charge density. It was pointed out that these two charged conditions represent two limiting cases for the case the surface charge of an entity arises from surface dissociation reactions (Krozel and Saville, 1992; Carnie and Chan, 1993a,b; Carnie et al., 1994a,b). Constant surface potential and constant surface charge density correspond respectively to the cases when the rate of dissociation reaction is infinitely fast and that is infinitely slow.

2. Theory

Let us consider the problem illustrated in Fig. 1 where a non-conductive spheroidal particle is placed on the axis of an infinitely long, non-conducting and uncharged cylindrical pore of radius b. The cylindrical coordinates (r,θ,z) with its origin located at the center of the particle are adopted. Let $2a$ and $2d$ be respectively the axis length of the particle in r- and in z-direction. Note that if $d/a > 1$, the particle is a prolate spheroids (needle-like), if $d/a=1$, it is spherical, and if $d/a < 1$, it is an oblate spheroids (disk-like). A uniform electric field $\boldsymbol{E}$ is applied in the z-direction, and the particle moves along the axis of the cylindrical pore. The axisymmetric nature of the present problem suggests that only the (r,z) domain needs to be considered. Based on the Gauss law, it can be shown that the spatial variation of the electrical potential $\boldsymbol{\Psi}$ is governed by the Poisson–Boltzmann equation

$$\nabla^2\boldsymbol{\Psi} = -\frac{\rho}{\varepsilon} = -\sum_{j=1}^{N}\frac{z_j e n_{j0}\exp(-z_j e\boldsymbol{\Psi}/k_B T)}{\varepsilon}, \tag{1}$$

where ∇^2 is the Laplace operator, ε is the permittivity of the liquid phase, ρ is the space charge density, N is the number of ionic species, n_{j0} and z_j are respectively the bulk number concentration and the valence of ionic species j, e is the elementary charge, k_B is the Boltzmann constant, and T is the absolute temperature. For convenience, the electrical potential $\boldsymbol{\Psi}$ is decomposed into the potential in the absence of the applied electric field, $\boldsymbol{\Psi}_1$, and the electrical potential outside the particle that arises from the applied field, $\boldsymbol{\Psi}_2$ (Henry, 1931). The applied electric field is weak so that the effect of double layer polarization is negligible. Suppose that the surface potential of particle is low, and, therefore, $\boldsymbol{\Psi}_1$ can be described approximately by

$$\nabla^2\boldsymbol{\Psi}_1 = \kappa^2\boldsymbol{\Psi}_1, \tag{2}$$

where $\kappa = (e^2\sum_j^N z_j^2 n_{j0}/\varepsilon k_B T)^{1/2}$ is the reciprocal Debye length. Similarly, the electrical potential associated with the applied electric field, $\boldsymbol{\Psi}_2$, is described by

$$\nabla^2\boldsymbol{\Psi}_2 = 0. \tag{3}$$

Two kinds of boundary conditions are considered. In the first kind the surface of the particle is maintained at constant electrical potential, and the boundary conditions for the electrical field are

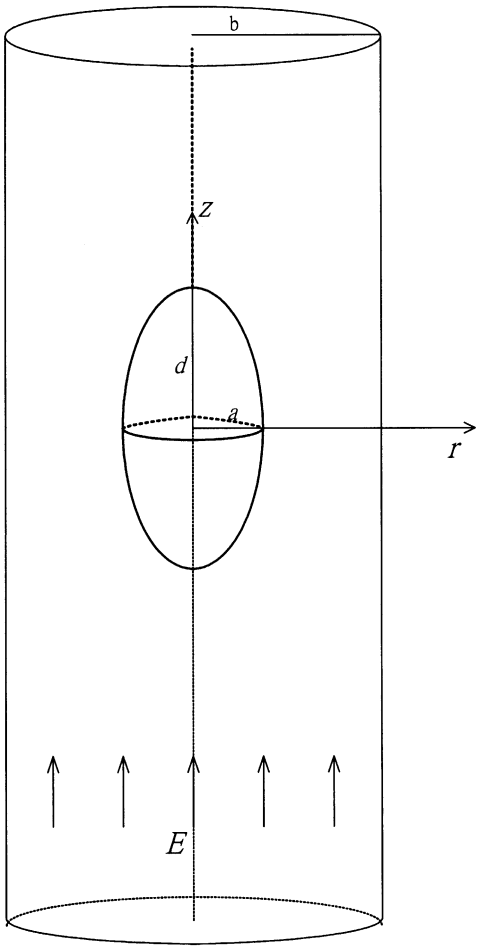

Fig. 1. Schematic representation of the problem considered. A spheroidal particle is placed on the axis of an infinitely long, uncharged cylindrical pore of radius b. An electric field $\boldsymbol{E}$ parallel to the axis of the pore is applied. The cylindrical coordinates (r,θ,z) are adopted. $2a$ and $2d$ are respectively the lengths of the axes of the particle in r- and z-direction.

$$\boldsymbol{\Psi}_1 = \zeta_a, \quad \boldsymbol{n}\cdot\nabla\boldsymbol{\Psi}_2 = 0 \quad \text{on particle surface,} \tag{4}$$

$$\frac{\partial\boldsymbol{\Psi}_1}{\partial r} = 0, \quad \frac{\partial\boldsymbol{\Psi}_2}{\partial r} = 0, \quad r = b, \tag{5}$$

$$\boldsymbol{\Psi}_1 = 0, \quad \nabla\boldsymbol{\Psi}_2 = -\boldsymbol{E}, \quad |z|\to\infty, \ r < b, \tag{6}$$

where ζ_a is the electrical potential on particle surface and $\boldsymbol{n}$ is the unit normal directed into the liquid phase. In the second kind, the surface of the particle is maintained at constant charge density, and the boundary conditions for the electrical field are

$$\boldsymbol{n}\cdot\nabla\boldsymbol{\Psi}_1 = \frac{-\sigma_a}{\varepsilon}, \quad \boldsymbol{n}\cdot\nabla\boldsymbol{\Psi}_2 = 0 \quad \text{on particle surface,} \tag{7}$$

$$\frac{\partial \Psi_1}{\partial r} = 0, \quad \frac{\partial \Psi_2}{\partial r} = 0, \quad r = b, \tag{8}$$

$$\Psi_1 = 0, \quad \nabla \Psi_2 = -\boldsymbol{E}, \quad |z| \to \infty, \ r < b, \tag{9}$$

where σ_a is the charge density on particle surface.

Suppose that the flow field can be described by the Navier–Stokes equation in the creeping flow regime. We have

$$\eta \nabla^2 \boldsymbol{u} - \nabla p = \rho \nabla \Psi, \tag{10}$$

$$\nabla \cdot \boldsymbol{u} = 0. \tag{11}$$

In these expressions, $\boldsymbol{u}$, η, and p are respectively the velocity, the viscosity, and the pressure of the liquid phase. Here, we assume the liquid phase is incompressible and has constant physical properties. Also, both the surface of particle and that of pore are no-slip (Backstrom, 1999). Then boundary conditions associated with Eqs. (10) and (11) are

$$\boldsymbol{u} = U \boldsymbol{i}_z \quad \text{on particle surface,} \tag{12}$$

$$\boldsymbol{u} = 0, \quad r = b \quad \text{and} \quad |z| \to \infty, \ r < b, \tag{13}$$

$$\boldsymbol{n} \cdot \nabla p = \boldsymbol{n} \cdot (\eta \nabla^2 \boldsymbol{u} - \rho \nabla \Psi) \quad \text{on particle surface,}$$

$$r = b \quad \text{and} \quad |z| \to \infty, \ r < b. \tag{14}$$

Here, $\boldsymbol{i}_z$ is the unit vector in the z-direction.

In our case, the forces acting on the particle include the hydrodynamic force and the electrostatic force. The axisymmetric nature of the geometry considered implies that only the forces in the z-direction need to be calculated. The electrostatic force acting on the particle in the z-direction, F_E^z, can be evaluated by

$$F_E^z = \int\int_S \sigma \, E_Z \, \mathrm{d}S = \int\int_S \sigma \left(-\frac{\partial \Psi}{\partial z} \right) \mathrm{d}S, \tag{15}$$

where S represents particle surface. The hydrodynamic force acting on the particle in the z-direction, F_D^Z, comprises the force arising from the viscous force, and that arising from the hydrodynamic pressure (Backstrom, 1999). We have, in mathematical expression,

$$F_D^Z = \int\int_S \eta \frac{\partial (\boldsymbol{u} \cdot \boldsymbol{t})}{\partial n} t_z \, \mathrm{d}S + \int\int_S -p n_z \, \mathrm{d}S. \tag{16}$$

Here, $\boldsymbol{t}$ and $\boldsymbol{n}$ are the unit tangential and unit normal vectors on particle surface, respectively, n is the magnitude of $\boldsymbol{n}$, and t_z and n_z are the z-component of $\boldsymbol{t}$ and that of $\boldsymbol{n}$ respectively. At steady state, the net force acting on a particle vanishes, that is,

$$F_D^Z + F_E^Z = 0. \tag{17}$$

The electrophoretic mobility of a particle is estimated by a trial-and-error procedure. An arbitrary particle velocity is guessed, and the equations governing the flow field and the electric field are solved numerically subject to the associated boundary conditions. The electric force and the viscous force experienced by the particle are then calculated, and the results substituted into Eq. (17) to see if it is satisfied. If it is not satisfied, then a new particle velocity is assumed, and the above procedure is repeated. FlexPDE (version 2.22, PDE Solutions Inc., USA), a differential equation solver, which is based on a finite element method, is adopted to solving the governing equations for the flow and the electric fields. The applicability and the accuracy of this software was examined previously (Hsu and Kao, 2002) by using it to solve the electrophoresis of a sphere along the axis of a cylindrical pore, and comparing the result obtained with those of Ennis and Anderson (1997) and Shugai and Carnie (1999). The former is based on a reflection method, which is unreliable if the ratio (particle radius/pore radius) is large. On the other hand, the latter used a numerical approach, which is inaccurate if the ratio (particle radius/pore radius) is small. Hsu and Kao (2002) concluded that the performance of the present numerical procedure was satisfactory regardless of the magnitude of the ratio (particle radius/pore radius).

3. Results and discussion

For a more concise presentation, the scaled electrophoretic mobility, ω, defined below is used in subsequent discussions:

$$\omega = \frac{U\eta}{\varepsilon \zeta_{\mathrm{ref}} E}, \tag{18}$$

where ζ_{ref} is a reference potential; for the case of constant surface potential ζ_{ref} is the particle surface potential ζ_a, and for the case of constant surface charge density ζ_{ref} is $k_B T/e$.

Solving Eqs. (2) and (3) subject to boundary conditions specified in Eqs. (4)–(6) or (7)–(9) gives the electric field, and solving Eqs. (10) and (11) subject to boundary conditions specified in Eqs. (12)–(14) gives the flow field. Figs. 2 and 3 show the typical electrical and flow fields obtained.

3.1. Constant surface potential

Fig. 4 shows the variation of the scaled electrophoretic mobility of a particle ω as a function of particle aspect ratio d/a for the case when its surface potential is constant. Both the result for the case when a is fixed and that when particle volume is fixed are presented. Fig. 4 reveals that for both the case when a is fixed and the case when particle volume is fixed, ω increases with d/a first, passing through a maximum, and then decreases with a further increase in d/a. As shown in Fig. 5, when a is fixed, a large d/a implies a large particle surface area, and the amount of charge on its surface is large, which yields a great electric force acting on it, and its mobility becomes large. On the other hand, as the surface area of a particle becomes large, the viscous force acting on its surface also becomes large, which has the effect of reducing its mobility. The situation for the case when particle volume is fixed is more complicated than that for

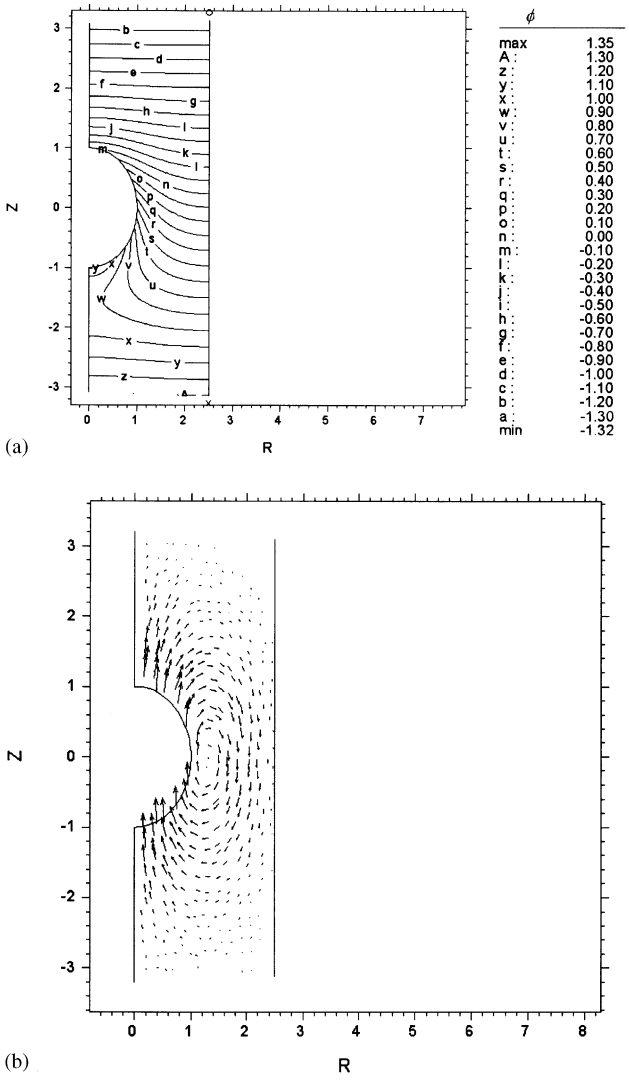

Fig. 2. Typical results for the electric field $\phi = e\psi/k_BT$, and flow field $\boldsymbol{u}^* = \boldsymbol{u}/U$, (b), for the case of constant surface potential with $\lambda = 0.4$ and ζ_a^* $(=\zeta_a/(k_BT/e)) = 0.5$.

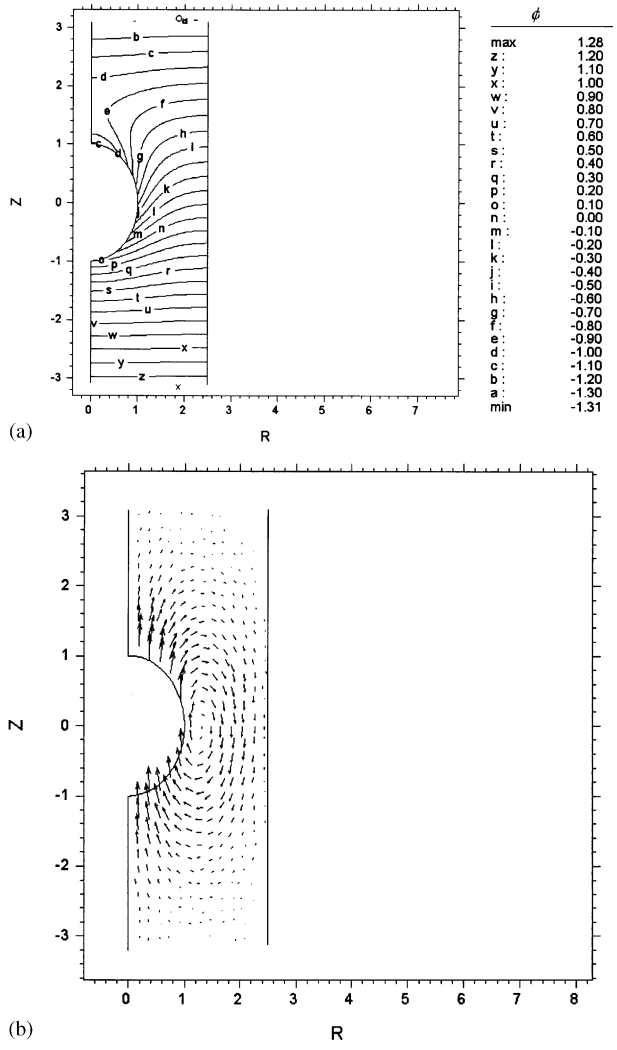

Fig. 3. Typical results for the electric field $\phi = e\psi/k_BT$, (a), and flow field $\boldsymbol{u}^* = \boldsymbol{u}/U$, (b), for the case of constant surface charge density with $\lambda = 0.4$ and σ_a^* $(=\sigma_a/(\varepsilon\kappa k_BT/e)) = -1$.

the case a is fixed. This is because ω is now influenced by both the viscous force acting on a particle and the thickness of double layer surrounding it. As illustrated in Fig. 5, when particle volume is fixed if $d/a < 1$ (oblate), the surface area of a particle decreases with the increase in d/a. It reaches a minimum at $d/a = 1$ (sphere), and then increases with a further increase in d/a for $d/a > 1$ (prolate). Because the viscous force acting on a particle is proportional to its surface area, ω increases with d/a when d/a is small. As d/a becomes large, a is small, and because λ is fixed, b is small too. Since the thickness of the double layer surrounding the particle is fixed, the larger the d/a the easier for the double layer to touch the wall of the cylindrical pore, the more significant the boundary effect, which is disadvantageous to the movement of the particle, and ω becomes smaller. The special behavior of ω for the case when particle volume is fixed is the net result of these effects.

The variation of the scaled electrophoretic mobility of a particle ω as a function of λ $(=a/b)$ at various particle aspect ratio d/a when its surface potential is constant is illustrated in Fig. 6. Both the results for the case a is fixed and those for the case when particle volume is fixed are presented. Note that in Fig. 6(a), both a and b are fixed, and in Fig. 6(b), b varies with a. Fig. 6 indicates that for a fixed d/a, ω decreases with the increase in λ. This is expected because the larger the λ, the closer the particle to the wall of the cylinder, and the more significant the hydrodynamic retardation arising from the presence of the latter. Note that if λ is small, the electrophoretic mobility of a prolate $(d/a > 1)$ is larger than that of an oblate $(d/a < 1)$, but the reverse is true if λ is large. This is because if λ is small, the wall effect is relatively unimportant. In this case, if a is fixed, a large d/a implies a large particle surface area, and therefore, a large amount of surface charge, which yields a great electric force

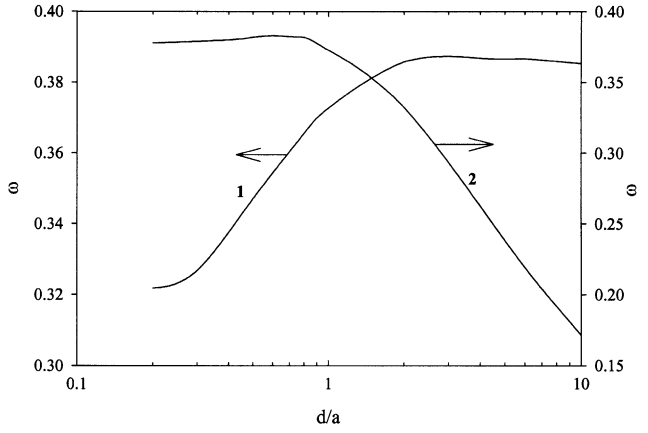

Fig. 4. Variation of scaled electrophoretic mobility ω $(=U\eta/\zeta_a E\varepsilon)$ as a function of particle aspect ratio d/a for the case of constant surface potential with $\lambda = 0.4$ and ζ_a^* $(=\zeta_a/(k_B T/e)) = 0.5$. Curve 1, a is fixed, 2, particle volume is fixed. Curve 1, $\kappa a = 1, 2$, $\kappa a = (d/a)^{-1/3}$.

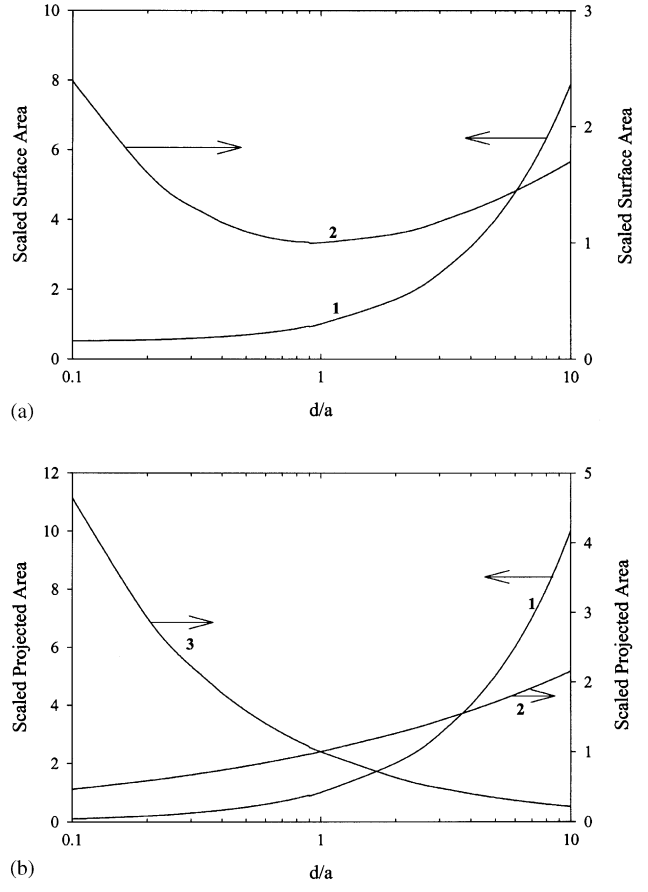

Fig. 5. (a) Variations of the ratio (surface area of a particle/that when $d/a = 1$) as a function of particle aspect ratio d/a. (b) Variation of the ratio (surface area of a particle projected onto a plane parallel to z-axis/that when $d/a = 1) = \pi ad/\pi a_0^2$, a_0 being the radius of the particle when $d/a = 1$, as a function of particle aspect ratio d/a. Curve 1, a is fixed, 2, particle volume is fixed. Curve 3 in part (b) is the variation of the ratio (surface area of a particle projected onto a plane perpendicular to z-axis/that when $d/a = 1) = \pi a^2/\pi a_0^2$ when particle volume is fixed.

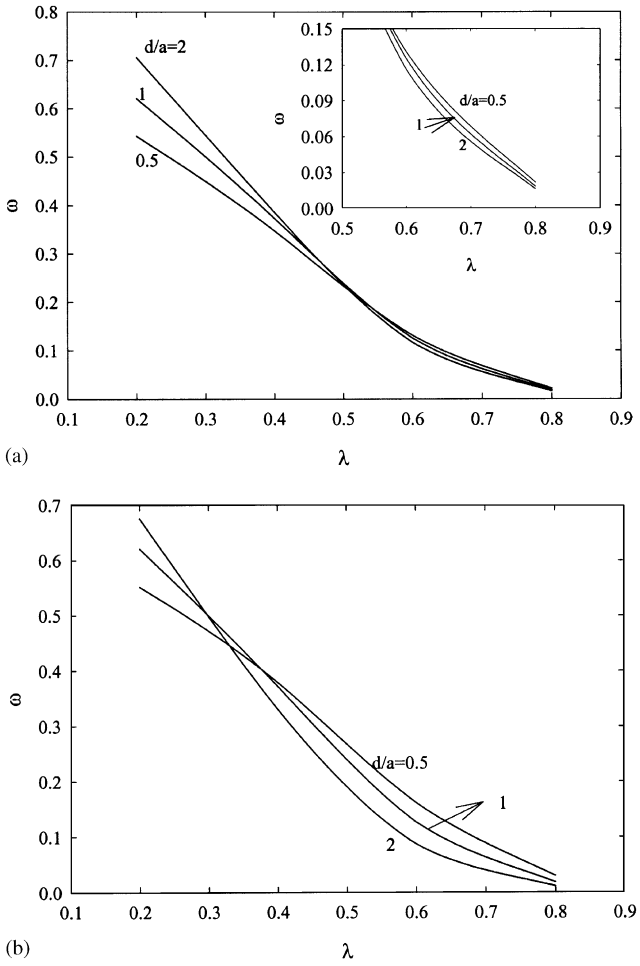

Fig. 6. Variation of scaled electrophoretic mobility ω as a function of λ at various particle aspect ratio a/d for the case of constant surface potential with $\zeta_a^* = 0.5$ and $\kappa a = 1$. (a) a is fixed, (b) particle volume is fixed.

acting on the particle, and its mobility becomes large. On the other hand, if λ is large, the wall effect becomes significant. In this case, the hydrodynamic retardation is mainly determined by the magnitude of the projected area of a particle on a plane parallel to the z-axis. Since the larger the d/a, the larger the projected area, as shown in Fig. 5(b), ω of a prolate becomes smaller than that of an oblate. When particle volume is fixed and λ is small, the hydrodynamic retardation on the movement of a particle is mainly determined by the magnitude of its projected area on a plane perpendicular to the z-axis. For a given λ, since particle volume is fixed, the smaller the d/a, the larger the a, and the larger the projected area is, as shown in Fig. 5(b), and therefore, ω of an oblate is smaller than that of a prolate. If λ is large, the wall effect becomes significant. As in the case when a is fixed, the hydrodynamic retardation is mainly determined by the magnitude of the projected area of a particle on a plane parallel to the z-axis. As shown in Fig. 5(b), because the larger the d/a, the larger the projected area, ω of a prolate becomes smaller than that of an oblate.

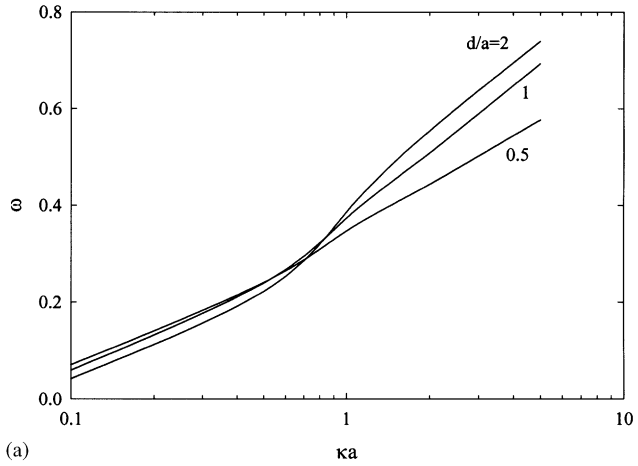

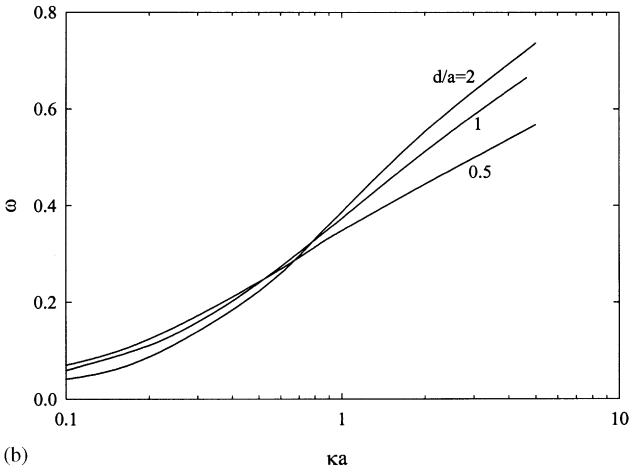

Fig. 7. Variation of scaled electrophoretic mobility ω as a function of κa at various particle aspect ratio a/d for the case of constant surface potential with $\lambda = 0.4$ and $\zeta_a^* = 0.5$. (a) a is fixed, (b) particle volume is fixed.

Fig. 7 illustrates the variation of the scaled electrophoretic mobility of a particle ω as a function of κa at various particle aspect ratio d/a when its surface potential is constant. Both the results for the case a is fixed and those for the case when particle volume is fixed are presented. Fig. 7 reveals that for a given d/a, ω increases with the increase in κa. This is expected since the larger the κa, the thinner the double layer surrounding a particle and the smaller the viscous retardation arising from its presence. As can be seen from Fig. 7(a), when a is fixed, if κa is small, ω of a prolate is smaller than that of an oblate, and the reverse is true if κa is large. This is because in Fig. 7(a) if κa is small, the double layer surrounding a particle is thick, and the wall effect is important. In this case, because the projected area of a prolate on a plane parallel to the z-axis is larger than that of an oblate, the viscous retardation of the former due to wall effect is greater than that of the latter, an oblate moves faster than a prolate. On the other hand, if κa is large, the double layer surrounding a particle is thin, the wall effect becomes unimportant. In this case the behavior of ω is similar to that

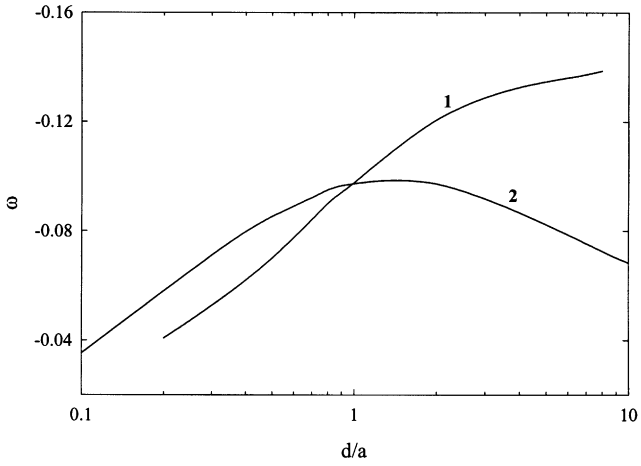

Fig. 8. Variation of scaled electrophoretic mobility ω as a function of particle aspect ratio d/a for the case of constant surface charge density with $\lambda = 0.4$ and $\sigma_a^* \ (=\sigma_a/(\varepsilon\kappa k_B T/e)) = -1$. Curve 1, a is fixed, 2, particle volume is fixed. Curve 1, $\kappa a = 1, 2$, $\kappa a = (d/a)^{-1/3}$.

shown in Fig. 6 for the case when λ is small, that is, ω is mainly controlled by the surface area of a particle and its projected area on a plane perpendicular to the z-axis. If a is fixed, since the surface area of a prolate is larger than that of an oblate, the electric force acting on the former is greater than that acting on the latter, and therefore, a prolate moves faster than an oblate. If particle volume is fixed, because the projected area of a prolate on a plane perpendicular to the z-axis is smaller than that of an oblate, as shown in Fig. 5(b), the hydrodynamic retardation of the former is smaller than that of the latter, and therefore, a prolate moves faster than an oblate.

3.2. Constant surface charge density

Fig. 8 shows the variation of the scaled electrophoretic mobility of a particle ω as a function of particle aspect ratio d/a for the case of constant surface charge density. Both the result for the case when a is fixed and that for the case when particle volume is fixed are illustrated. Fig. 8 reveals that if a is fixed, $|\omega|$ increases monotonically with the increase in d/a for the range of d/a examined, which is different from the result when particle surface is maintained at a constant surface potential, as presented in curve 1 of Fig. 4. As in the case of constant surface potential the increase of $|\omega|$ with d/a arises from the increase in the amount of surface charge with d/a. The behavior of $|\omega|$ as d/a varies when particle volume is fixed is similar to that of ω for the case of constant surface potential shown in Fig. 4, and can be explained by the same reasoning.

The variation of the scaled electrophoretic mobility of a particle ω as a function of λ at various particle aspect ratio d/a for the case of constant surface charge density is illustrated in Fig. 9. Both the results for the case when a is fixed and those when particle volume is fixed are presented.

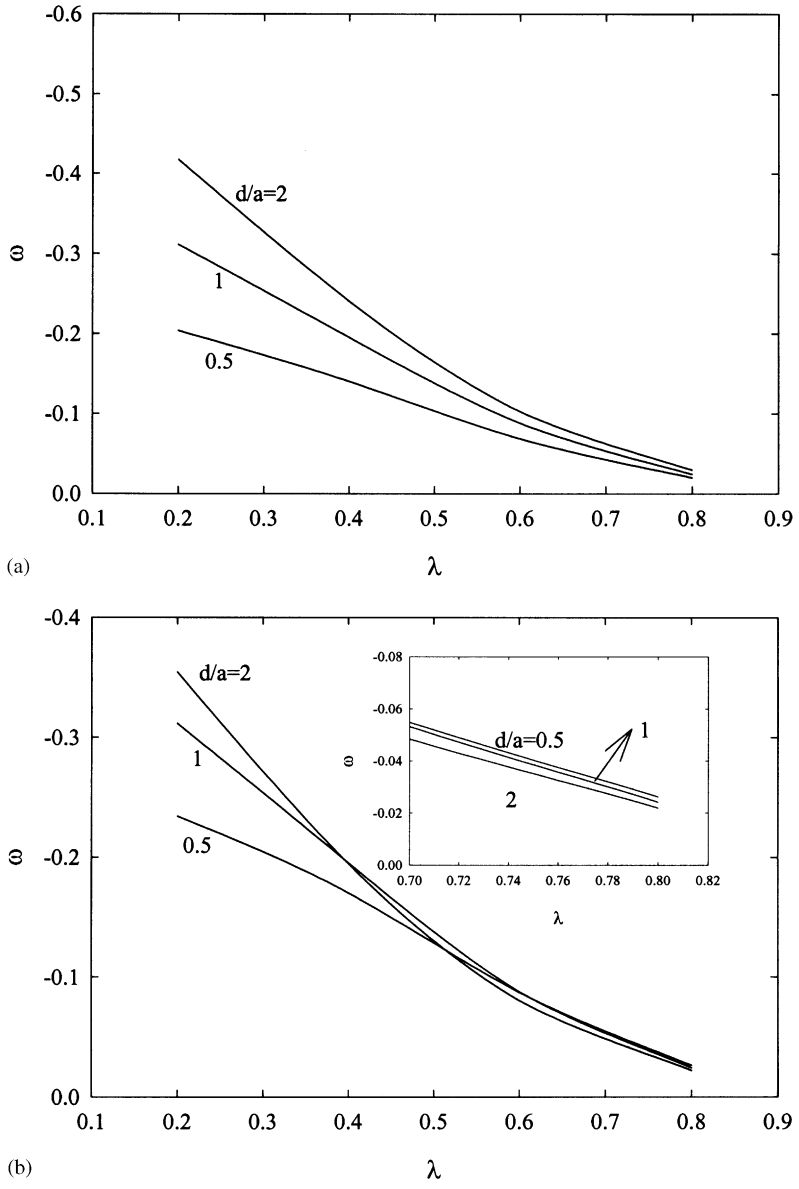

Fig. 9. Variation of scaled electrophoretic mobility ω as a function of λ at various particle aspect ratio a/d for the case of constant surface charge density with $\sigma_a^* = 1$ and $\kappa a = 1$. (a) a is fixed, (b) particle volume is fixed.

The trend of the absolute scaled mobility as λ varies is similar to the scaled mobility shown in Fig. 6, in which surface potential is constant, that is, $|\omega|$ decreases with the increase in λ, which is expected since the larger the λ the more significant the wall effect. Note that, however, when a is fixed, the curves correspond to different values of d/a do not cross each other as that observed in Fig. 6(a); $|\omega|$ of a prolate is always larger than that of an oblate for the range of λ examined. As can be seen in Fig. 9(b) if particle volume is fixed, the behavior of the absolute scaled mobility is similar to the scaled mobility shown in Fig. 6(b), in which surface potential is constant.

Fig. 10 illustrates the variation of the scaled electrophoretic mobility of a particle ω as a function of κa at various particle aspect ratio d/a for the case of constant surface charge density. Both the results for the case when a is fixed and those when particle volume is fixed are shown. Fig. 10 reveals that for a given d/a, $|\omega|$ increases monotonically with the increase in κa, which is similar to that observed Fig. 7, and can be explained by the same reasoning. However, the curves in Fig. 10 correspond to different values of d/a do not cross each other; $|\omega|$ of a prolate is always larger than that of an oblate.

The geometry considered in this study is an idealized one, where a spheroidal particle is moving along the axis of a cylindrical pore. In practice, the shape of a particle and its position, the direction of its movement, and the shape of boundary can all be arbitrary. In this case, the

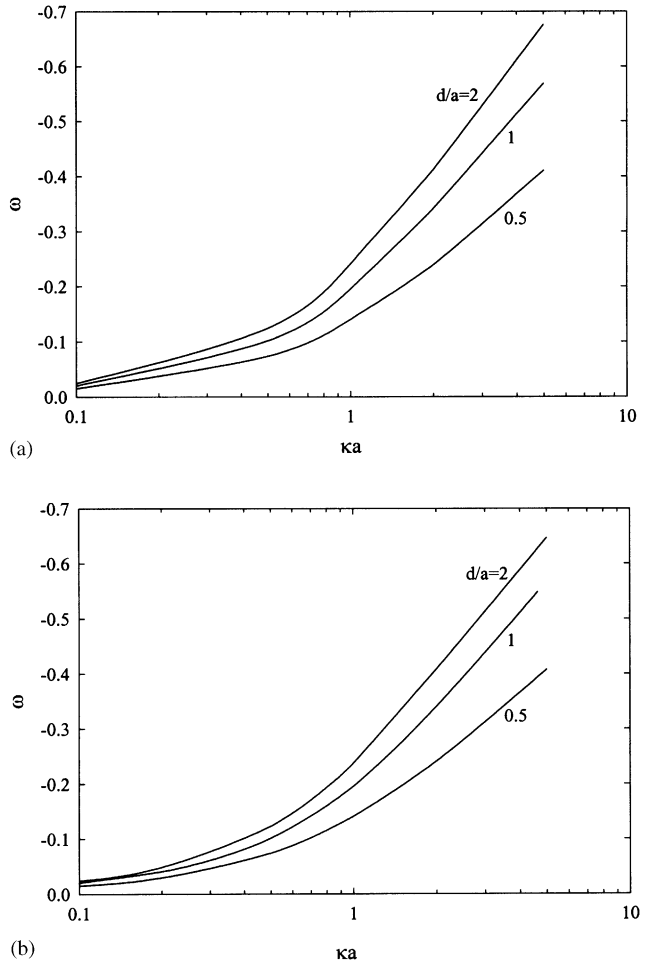

Fig. 10. Variation of scaled electrophoretic mobility ω as a function of κa at various particle aspect ratio a/d for the case of constant surface charge density with $\lambda=0.4$ and $\sigma_a^*=1$. (a) a is fixed, (b) particle volume is fixed.

electrophoresis problem is of complicated nature, and solving the governing equations subject to the associated boundary conditions becomes non-trivial, even if it is solved numerically. In general, an efficient three-dimensional numerical scheme for the resolution of a boundary-value problem needs to be developed.

4. Conclusions

In summary, the electrophoretic mobility of a spheroidal particle along the axis of a cylindrical pore is investigated. Using the geometry of the former has the advantage that it is capable of simulating a wide class of particles. We show that for the case when the wall effect is significant, which occurs if the double layer surrounding a particle is thick and/or the linear size in the direction perpendicular to its movement is large, the projected area of the particle on a plane parallel to its movement plays the key role in the determination of its electrophoretic behavior. On the other hand, if the wall effect is insignificant, the projected area of a particle on a plane perpendicular to its movement plays the key role. If the volume of a particle is fixed, its electrophoretic mobility exhibits a local maximum as its aspect ratio varies, which is observed in both the case when particle surface is maintained at a constant potential and when it is maintained at a constant charge density. When the linear size of a particle in the direction perpendicular to its movement is fixed, its electrophoretic mobility has a local maximum as particle aspect ratio varies if its surface is maintained at a constant potential, but the local maximum is not observed if its surface is maintained at a constant charge density. For a fixed particle volume, the relative magnitudes of the electrophoretic mobility of prolate, sphere, and oblate depend on the degree of wall effect. If the wall effect is important, it follows the order prolate $<$ sphere $<$ oblate, and the reverse is true if the wall effect is unimportant.

Notation

a	half axis length of particle r-direction, m
b	radius of cylindrical pore, m
d	half axis length of particle in z-direction, m
e	elementary charge, C
$\boldsymbol{E}$	electric field, V m^{-1}
F_E^z	electrostatic force acting on particle in z-direction, N
F_D^z	hydrodynamic force acting on particle in z-direction, N
$\boldsymbol{i}_z$	unit vector in z-direction, dimensionless
k_B	Boltzmann constant, J K^{-1}
$\boldsymbol{n}$	unit normal vector on particle surface, dimensionless
n	magnitude of $\boldsymbol{n}$, dimensionless
n_z	z-component of $\boldsymbol{n}$, dimensionless
n_{j0}	bulk number concentration of ionic species j, m^{-3}
N	number of ionic species, dimensionless
p	pressure, Pa
S	particle surface, m^2
$\boldsymbol{t}$	unit tangential vectors on particle surface, dimensionless
t_z	z-component of $\boldsymbol{t}$, dimensionless
T	absolute temperature, K
$\boldsymbol{u}$	velocity of liquid phase, m s^{-1}
$\boldsymbol{u}^*$	scaled velocity of liquid phase, dimensionless
z_j	valence of ionic species j, dimensionless

Greek letters

ε	permittivity of liquid phase, C^2 N^{-1} m^{-2}
∇	gradient operator, m^{-1}
ζ_{ref}	reference potential, V
ζ_a	electrical potential on particle surface, V
η	viscosity of liquid phase, kg m^{-1} s^{-1}
κ	reciprocal Debye length, m^{-1}
ρ	space charge density, C m^{-3}

σ_a charge density on particle surface, C m^{-1}
ϕ scaled electrical potential, dimensionless
Ψ electrical potential, V
Ψ_1 potential in the absence of applied electric field, V
Ψ_2 electrical potential outside particle that arises from applied electric field, V

Acknowledgements

This work is supported by the National Science Council of the Republic of China.

References

Backstrom, G., 1999. Fluid Dynamics by Finite Element Analysis. Studentlitteratur, Sweden.

Carnie, S.L., Chan, D.Y.C., 1993a. Interaction free energy between identical spherical colloidal particles: the linearized Poisson–Boltzmann theory. Journal of Colloid and Interface Science 155, 297–312.

Carnie, S.L., Chan, D.Y.C., 1993b. Interaction free energy between plates with charge regulation: a linearized model. Journal of Colloid and Interface Science 161, 260–264.

Carnie, S.L., Chan, D.Y.C., Gunning, J.S., 1994a. Electrical double layer interaction between dissimilar spherical colloidal particles and between a sphere and a plate: the linearized Poisson–Boltzmann theory. Langmuir 10, 2993–3009.

Carnie, S.L., Chan, D.Y.C., Stankovich, J., 1994b. Computation of forces between spherical colloidal particles: nonlinear Poisson–Boltzmann theory. Journal of Colloid and Interface Science 165, 116–128.

Chen, S.B., Keh, H.J., 1992. Axisymmetric electrophoresis of multiple colloidal spheres. Journal of Fluid Mechanics 238, 251–276.

Chih, M.H., Lee, E., Hsu, J.P., 2002. Electrophoresis of a sphere normal to a plane at arbitrary electrical potential and double layer thickness. Journal of Colloid and Interface Science 248, 383–388.

Chu, J.W., Lin, W.H., Lee, E., Hsu, J.P., 2001. Electrophoresis of a sphere in a spherical cavity at arbitrary electrical potentials. Langmuir 17, 6289–6297.

Ennis, J., Anderson, J.L., 1997. Boundary effects on electrophoretic motion of spherical particles for thick double layers and low zeta potential. Journal of Colloid and Interface Science 185, 497–514.

Feng, J.J., Wu, W.Y., 1994. Electrophoretic motion of an arbitrary prolate body of revolution toward an infinite conducting wall. Journal of Fluid Mechanics 264, 41–58.

Henry, D.C., 1931. The cataphoresis of suspended particles. Part I. The equation of cataphoresis. Proceedings of the Royal Society of London Series A 133, 106–129.

Hsu, J.P., Kao, C.Y., 2002. Electrophoresis of a finite cylinder along the axis of a cylindrical pore. Journal of Physical Chemistry B 106, 10605–10609.

Hunter, R.J., 1989. Foundations of Colloid Science, Vol. I. Clarendon Press, Oxford.

Keh, H.J., Anderson, J.L., 1985. Boundary effects on electrophoretic motion of colloidal spheres. Journal of Fluid Mechanics 153, 417–439.

Keh, H.J., Chen, S.B., 1988. Electrophoresis of a colloidal sphere parallel to a dielectric plane. Journal of Fluid Mechanics 194, 377–390.

Keh, H.J., Chen, S.B., 1989a. Particle interactions in electrophoresis: I. Motion of two spheres along their line of centers. Journal of Colloid and Interface Science 130, 542–555.

Keh, H.J., Chen, S.B., 1989b. Particle interactions in electrophoresis: II. Motion of two spheres normal to their line of centers. Journal of Colloid and Interface Science 130, 556–567.

Keh, H.J., Chiou, J.Y., 1996. Electrophoresis of a colloidal sphere in a circular cylindrical pore. American Institute of Chemical Engineers Journal 42, 1397–1406.

Keh, H.J., Jan, J.S., 1996. Boundary effects on diffusiophoresis and electrophoresis: motion of a colloidal sphere normal to a plane wall. Journal of Colloid and Interface Science 183, 458–475.

Keh, H.J., Lien, L.C., 1989. Electrophoresis of a dielectric sphere normal to a large conducting plane. Journal of the Chinese Institute of Chemical Engineers 20, 283–290.

Keh, H.J., Lien, L.C., 1991. Electrophoresis of a colloidal sphere along the axis of a circular orifice or a circular disk. Journal of Fluid Mechanics 224, 305–333.

Keh, H.J., Yang, F.R., 1990. Particle interactions in electrophoresis: III. Axisymmetric motion of multiple spheres. Journal of Colloid and Interface Science 139, 105–116.

Keh, H.J., Horng, K.D., Kuo, J., 1991. Boundary effects on electrophoresis of colloidal cylinders. Journal of Fluid Mechanics 231, 211–228.

Krozel, J.W., Saville, D.A., 1992. Electrostatic interactions between two spheres: solutions of the Debye–Hückel equation with a charge regulation boundary condition. Journal of Colloid and Interface Science 150, 365–373.

Lee, E., Chu, J.W., Hsu, J.P., 1997. Electrophoretic mobility of a spherical particle in a spherical cavity. Journal of Colloid and Interface Science 196, 316–320.

Lee, E., Chu, J.W., Hsu, J.P., 1998. Electrophoretic mobility of a sphere in a spherical cavity. Journal of Colloid and Interface Science 205, 65–76.

Loewenberg, M., Davis, R.H., 1995. Near-contact electrophoretic particle motion. Journal of Fluid Mechanics 288, 103–122.

Morrison, F.A., 1970. Electrophoresis of a particle of arbitrary shape. Journal of Colloid and Interface Science 34, 210–214.

Shugai, A.A., Carnie, S.L., 1999. Electrophoretic motion of a spherical particle with a thick double layer in bounded flows. Journal of Colloid and Interface Science 213, 298–315.

Shugai, A.A., Carnie, S.L., Chan, D.Y.C., Anderson, J.L., 1997. Electrophoretic motion of two spherical particles with thick double layers. Journal of Colloid and Interface Science 191, 357–371.

Sun, K.L., Wu, W.Y., 1995. Electrophoresis of two arbitrary axisymmetric prolate particles. International Journal of Multiphase Flow 21, 705–714.

Tang, Y.P., Chih, M.H., Lee, E., Hsu, J.P., 2001. Electrophoretic motion of a charge-regulated sphere normal to a plane. Journal of Colloid and Interface Science 242, 121–126.

Zydney, A.L., 1995. Boundary effects on the electrophoretic motion of a charged particle in a spherical cavity. Journal of Colloid and Interface Science 169, 476–485.